A Solution to the Forward Problems by Green Functions in New Fluorescence Molecular Tomography Imaging System

Toktam Jahanfar[1,2], Sedighe Marjaneh Hejazi[1,2*] , Amir Homaun Jafari[1,2], Hanieh Mohammadreza[1,2]

1. Department of Medical Physics and Biomedical Engineering, Tehran University of Medical Sciences, Tehran, Iran.
2. Research Center of Cellular and Molecular Imaging, Tehran University of Medical Sciences, Tehran, Iran.

Article info:
Received: September 29 2012
Accepted: March 03 2013

Keywords:
Fluorescence Molecular Tomography,
Forward Problem,
Green Function,
Born Approximation,
Iterative Approach.

A B S T R A C T

Purpose: Optical imaging is established as one of the modalities applied to molecular imaging studies. Molecular imaging can be used to visualization of molecular events in the cellular or sub-cellular level. One of the main goals in optical imaging is giving source distribution. The Forward problem seeks to determine the photon density on the surface of the subject. Among the different methods, Green functions provide a fast method for modeling the diffusion. Green functions are different depending on the source shape, set up and geometry.

Methods: In this study, a new optical set up was implemented in the cylindrical geometry. The software is developed and written in MATLAB programming to estimate the intensity on the object's surface. The algorithm is based on diffusion approximation and evaluated by phantom experiment.

Results: The results showed significant correlation coefficients (R >0.9) which demonstrated the high accuracy of the algorithm.

Conclusion: We have presented an approximate algorithm that solves the 3D diffusion equation in homogeneous turbid phantom like tissue. The algorithm can be used as part of the reconstruction program using FMT.

1. Introduction

Fluorescence molecular imaging is a non-invasive technique to visualize biological process at cellular and sub-cellular levels, which is widely used in clinical fields such as small animal imaging. In particular, fluorescence molecular tomography (FMT) is applied for localizing and quantifying specimens labeled by the fluorescent nanoparticles. FMT is accomplished by irradiation of the sample with lasers and collection of fluorescent light emitted in all 360 angles. The distribution of the fluorochrome concentration within the sample is obtained by the reconstruction of obtained fluorescent intensity,. The problem of reconstructing map of the fluorescent concentration from the interior of a turbid medium can be divided into two steps: the forward and the inverse problem.

The forward problem of fluorescence tomography for a given 3D source distribution seeks to determine the photon density on the surface of a media. In fact, the forward models the transition radiation inside the media. Using the results of this step, the inverse problem or reconstruction of obtained intensity is undertaken. Obviously, the final step would be incorrect with a non-exact solution in the forward problem. Existing methods for modeling light transport are either deterministic based on the solutions to governing equations [1], or stochas-

**** Corresponding Author:***
Sedighe Marjaneh Hejazi, PhD
Department of Medical Physics and Biomedical engineering, Tehran University of Medical Sciences, Tehran, Iran.
Tel: +98 21 66907527
E-mail: mhejazi@sina.tums.ac.ir

tic based on simulations of the individual scattering and absorption event undertaken by each photon [2].

A general model of light propagation can be developed using the radiative transfer equation (RTE), but a simpler model that can be derived from this equation in the case of sufficiently high scattering, which has had a high degree of success, is the diffusion equation [3]. The advantage of diffusion equation is using analytical solutions for a variety of geometries. Analytical solutions can be obtained for a variety of geometries. Methods for solving the diffusion equation include analytical expressions based on Green functions [4], and numerical methods based on finite difference methods (FDM) or finite element methods (FEM) [5]. Green function techniques are now commonly used to solve the forward problem for image reconstruction, particularly for fast imaging techniques where the geometry can be approximated as a slab or an infinite half-space, such as for optical topography[6]. Analytical solutions of the diffusion equation were found, e.g. for infinite [7], semi-infinite [8], slab geometries[9], and for a sphere [4, 10], a cylinder [4, 10, 11], as well as for inhomogeneous geometries [12].

In recent years, this approach has been extended. Kim et al. [13], has devised a method for calculating the Green functions as an expansion into plane-wave solutions which allows analytical solutions for the diffusion equation or the RTE to be derived. Also, Ripoll et al. used the Kirchhoff approximation which models the Green function between two points in a medium of arbitrary geometry as a sum of the infinite space Green functions as well as other Green functions calculated for diffusive waves which are multiply reflected off the boundary [14].

For tomographic imaging of the fluorescence distribution, the Born approximation is a well-known perturbation technique that allows us to generate an analytical solution to the diffusion equation and has been used in diffuse optical tomography [15].

In this study, we focus on the forward problem, which is accounted Green function for the modeling of light propagation and determining 3D distribution fluorescence intensity on the object surface in a new FMT imaging system. We developed a forward modeling algorithm based on the Born approximation for a new FMT imaging system. We have used our algorithm for a cylinder phantom with a cylinder fluorescent source. Finally, we present the results of fluorescent phantom study to compare the performance of our model with an experimental data.

2. Material and Methods

2.1. Experimental Setup

To implement 360–degree projections FMT, a free-space system was developed as shown in Fig. 2.

Figure 1. The new Fluorescence Molecular Tomography system; FMT is a free-space system that applied for localizing and quantifying specimens labeled by the fluorescent nanoparticles.

Three wavelength constant waves (CW) laser beams are directed toward the sample by using a scanner and radiate into a vertical sample which is placed on the thin anti-reflection plate in the central part of system. The scanner has the capability for scanning the sample in the area of a 3×3 square. The laser which irradiated the sample contained the fluorescent materials. Fluorescent light transmitted through the diffuse medium was, then, recorded by the charge coupled device (CCD) camera at both the excitation and fluorescent wavelengths using appropriate filters. The CCD has the ability to rotate around the sample.

For experimental evaluation, we made a 2-cm diameter cylinder phantom. The phantom was made from 1 (g) agarose (BioGene, Kimbolton, UK), 4 (ml) intralipid 20% (Fresenius SE, Bad Homburg, Germany) and 3 (micro liter) Indian ink (PelikanHolding, Schindellegi, Switzerland) [16] dissolved in 100 ml water. The reduced scattering and absorption coefficients, at 692 nm, were then found to be μ'_s and μ_a equal to 8 cm^{-1} and 0.11 cm^{-1} respectively [17].

There is a cylindrical hole with 3mm diameter in 0.5 cm distance from the axis and parallel in middle of the phantom. The hole contained quantum dot PL-QDN-660 (Plasma Chem., Germany, emission wavelength 660nm). The optical images were recorded for every 10 degrees and 6 projections in each angle.

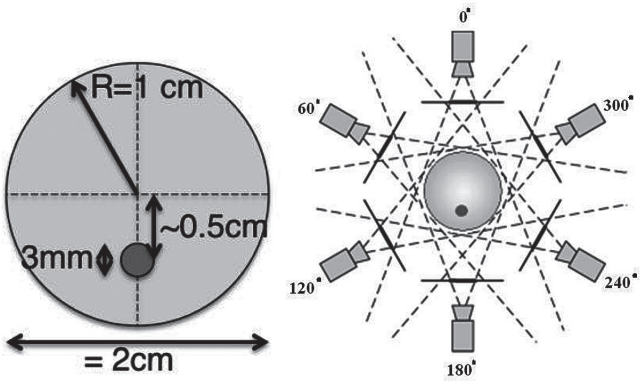

Figure 2. Geometry used for study. A 2-cm diameter cylinder with a 3mm diameter cylindrical hole in 0.5 cm distance from the cylinder axis.

2.2. Diffusion Approximation

The Forward problem is described by determination of light intensity at any position in the medium and consequently on the surface, *S*, by giving the light source distribution and distribution of the fluorescent concentration within volume *V*.

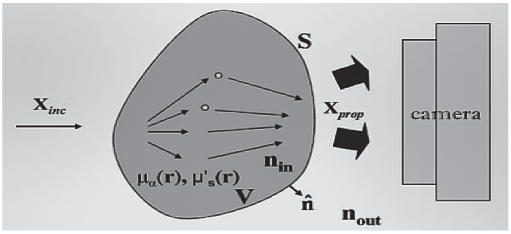

Figure 3. The propagation of light in finite homogenous media; light propagates diffusively in the media with the refractive index n_in and surrounded by a non-diffusive medium with refractive index n_out.

Light propagation in a highly scattering medium is well approximated by the diffusion equation [18].

$$-D\nabla^2 U(\boldsymbol{r},t) + \mu_a U(\boldsymbol{r},t) = S_0(\boldsymbol{r},t) \quad (1)$$

Where U is the average intensity at location r, $S0$ is an internal source of light in the medium, D and μ_a are the diffusion and absorption coefficient respectively. D is defined as,

$$\mathrm{D} = 1/(3\mu'_s + \mu_a) \quad (2)$$

that μ'_s is the reduced scattering coefficient [19].

An experimental set up based on fluorescence molecular imaging was designed and implemented. For this new system, the forward algorithm was written based on diffusion approximation in MATLAB (The Math Works Inc., Natick, MA, USA) programming.

2.3. The Forward Algorithm

The Forward algorithm was written based on the measurement of the light distribution *(U)* in an infinite homogeneous medium. The Green function *g* which satisfies [20]:

$$(\nabla^2 + k^2)g(k|r_s - r_d|) = -\delta(r_s - r_d) \quad (3)$$

Where *g* is the Green function,

$$(G(k|r_s - r_d|) = e^{ik|r_s - r_d|}/4\pi|r_s - r_d|) \quad (4)$$

and r_s and r_d represent the source and detector positions receptively. By definition of the Green function, the spatial distribution of intensity in an infinite homogeneous medium is given by [1]:

$$U(r) = \frac{1}{4\pi D}\int_v dV \frac{S(r)e^{-k_0|r - r_s|}}{|r - r_s|} \quad (5)$$

For solving the diffusion equation, the boundary condition should be considered [21]. The complete Green function inside the diffusive medium was found in terms of Green theorem [22].

$$G(\boldsymbol{r_s},\boldsymbol{r_d}) = g(k|\boldsymbol{r_s} - \boldsymbol{r_d}|) + \frac{1}{4\pi}\int_s [C_{nd} D\frac{\partial g(k|\boldsymbol{r'} - \boldsymbol{r_d}|)}{\partial \boldsymbol{n'}} + g(k|\boldsymbol{r_s} - \boldsymbol{r_d}|)]\frac{\partial G(\boldsymbol{r_s}.\boldsymbol{r'})}{\partial \boldsymbol{n'}} \quad (6)$$

$\partial/\partial n' = n'.\nabla_r'$ and n' is the surface unit outward normal pointing into the non-diffusive medium. The C_{nd} co-

efficient takes into account the refractive mismatch between both the media. For typical tissue/air index values (n_{in}=1.33, n=1) C_{nd}=5 [12]. The studies showed that numerical methods to solve Eq.6 require large computation times and the Kirrchhoff approximation method is also valid only at diffuse media bounded by convex surfaces and geometries that are larger than the decay length of the diffuse intensity (typically, R > 2.0 cm) [14].Therefore, to improve the applications of the analytical methods while maintaining favorable computation characteristics, we used the N-Order Diffuse-Reflection Boundary Method [23]. This method is based on approximation by using the Euler method with time step τ as

$$\mathbf{G}^{(N)}(\boldsymbol{r}_s,\boldsymbol{r}_k)=\boldsymbol{G}^{(N-1)}(\boldsymbol{r}_s,\boldsymbol{r}_k)-\tau.g(k|\boldsymbol{r}_s-\boldsymbol{r}_k|)+$$
$$\tau\frac{1}{4\pi}\sum_{p=1}^{N}\left[\frac{\partial g(k|\boldsymbol{r}_s-\boldsymbol{r}_k|)}{\partial \boldsymbol{n}_p}+\frac{1}{C_{nd}D}g(k|\boldsymbol{r}_s-\boldsymbol{r}_k|)\right]\times\boldsymbol{G}^{(N-1)}(\boldsymbol{r}_s,\boldsymbol{r}_k)\Delta S(\boldsymbol{r}_p) \quad (7)$$

Here we must take the principal value of the integral, i.e., exclude those points where the source and the detector coincide, and substitute those with the corresponding self-induction values which are depending on the medium and surface discretization area. The distribution of the average intensity in a finite homogeneous medium is given by,

$$U(r_d)=\frac{1}{4\pi}\int_v\frac{S(\boldsymbol{r}')}{D}G(\boldsymbol{r}',\boldsymbol{r}_d)d\boldsymbol{r}'\,\boldsymbol{r}_d\in V \quad (8)$$

Therefore, the solution of the diffusion equation for the fluorescent light is derived with replacing *S(r')*

with:

$$S_{fl}(r')=\Gamma N_e(r)=\eta\sigma_{fl}N_t(r)U_{exc}(r,r_s) \quad (9)$$

Where η is the fluorescence quantum yield and σ_{fl} the absorption cross section of the molecular at the excitation wavelength λ_{exc} . N_e and N_t are the number densities in the excited state and the total number density of the fluorescent molecules.

In general, the solution of the diffusion equation for the emission fluorescent light can be written as [1]:

$$U_{fl}(r_s,r)=\frac{\eta\sigma_{fl}S_{dc}}{16\pi^2D_{fl}D_{inc}}\int_v dV'G_{inc}(r',r_s)N_t(r')G_{fl}(r',r) \quad (10)$$

In Eq.10 G_{nc} and G_{fl} denote the homogenous Green functions for the excitation and fluorescence, respectively. The intensity, detected at emission wavelength, requires determination of the detector gain and gain factor associated with light-source strength for each source-detector's pixel. To obtain more-manageable expressions for the fluorescent, we used Born approximation. The Born field $U_{bo}(\vec{r_s},\vec{r_d})$ at the detectors' position $\vec{r_d}$ due to a source at position $\vec{r_s}$ is calculated by dividing measurements at the emission and excitation wavelengths, $U_{fl}(\vec{r_s},\vec{r_d})$ by $U_{inc}(\vec{r_s},\vec{r_d})$ [24]:

$$U_{Bo}(\vec{r}_s,\vec{r}_d)=\frac{1}{\Theta_f}\frac{U_{fl}(\vec{r}_s,\vec{r}_d)}{U_{inc}(\vec{r_s},\vec{r_d})} \quad (11)$$

In Eq.8, Θ_f is the filter attenuation factor. Born field significantly minimizes the sensitivity of the reconstruction to background heterogeneities and eliminates any position-dependent contributions [15].

To account for the noncontact measurements, we have used the non-contact equations that model free space propagation of diffuse waves [1]. The total power measured at the detector is obtained as

$$\Gamma(r_d,r_p)=\xi(r_d,r_p)\frac{f(NA-\sin\theta_d)}{|r_d-r_p|^2}(n_p.u_{r-r_d})(n_d.u_{r-r_d})dA \quad (12)$$

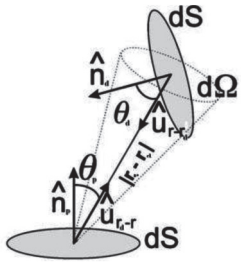

Figure 4. The propagation of light in free space; light propagates from an object surface with a normal n_s in free space and detected by detector with normal n_d.

Where Γ is a so-called transformation factor describing the contribution of the surface points onto a certain detector at position r_d with a detector normal n_d and area A[25].

$$\Gamma(r_d, r_p) = \xi(r_d, r_p) \frac{f(NA - \sin\theta_d)}{|r_d - r_p|^2} (n_p . u_{r-r_d})(n_d . u_{r-r_d}) dA \quad (13)$$

Where $\xi \in (0,1)$ is a factor discarding surface points not visible by the detector, NA is the numerical aperture which is modeled through a function f which describes a Gaussian of full width at halfmaximum of *2NA*. We evaluated our result with numerical and experimental methods.

3. Results

The modeling of light distribution in the media has been undertaken and Fig. 4(a) displays the intensityon surface of the cylindrical phantom by using the Born approximation. Figure 4(b) shows the result images of applying the forward algorithm in 0 degree where fluorescent source is in the maximum distance from the laser source.

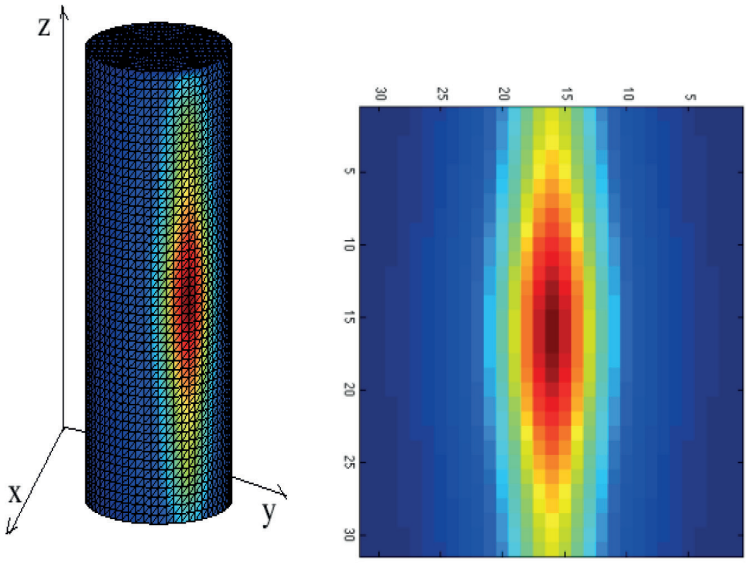

Figure 5. Result images; Recorded fluorescence intensity while detector located a) on the surface and b) case at certain distance in free space.

The modeling of recorded fluorescence intensity while the detector located on the surface, and in other cases at a certain distance in free space, was performed in every 30 degrees. Peak signal-to-noise ratio (PSNR) and average normalized intensities were calculated for each projection and results are shown in table 1.

The algorithm has been evaluated with numerical and experimental methods.

The results of average normalized intensity and PSNR in numerical method in the same ROI is given in table 2. Also, Mean Error (ME) and correlation between analytical and numerical methods is showed in every 30 degree.

For the sake of comparison, a correlation test and t-test were used. There was no significant difference between PSNR of analytical and similar results which were ob-

Table 1. Modeling results; Average normalized intensity modeled and Peak Signal to Noise Ratio (PSNR) in different degrees while detector located on the surface, and in free space.

Degree	Detector located in free space		Detector located on the surface	
	Average normalized intensity	PSNR (dB)	Average normalized intensity	PSNR (dB)
0	0.021	50.98	0.67	53.32
30	0.033	52.04	0.64	53.37
60	0.045	52.78	0.35	54.31
90	0.057	55.14	0.27	57.84
120	0.073	58.49	0.24	62.29
150	0.096	61.17	0.23	62.64
180	0.090	63.34	0.20	62.84
210	0.094	61.17	0.23	62.64
240	0.072	58.49	0.24	62.29
270	0.055	55.14	0.27	57.84
300	0.047	52.78	0.35	54.31
330	0.033	52.04	0.64	53.32

Table 2. The results of the average normalized intensity and Peak Signal to Noise Ratio (PSNR) in numerical method and Mean Error (ME) and the correlation between analytical and numerical methods in different degrees.

Degree	Average normalized intensity	PSNR(db)	ME(1>)	Correlation with analytical method
0	0.023	50.735	0.166	0.91
30	0.035	51.745	0.155	0.91
60	0.044	53.048	0.148	0.91
90	0.056	55.297	0.145	0.92
120	0.074	57.042	0.143	0.93
150	0.097	60.836	0.142	0.93
180	0.091	62.276	0.140	0.94
210	0.097	60.297	0.142	0.93
240	0.074	57.497	0.143	0.93
270	0.056	55.836	0.145	0.92
300	0.044	53.928	0.148	0.91
330	0.035	51.003	0.155	0.91

tained from the numerical method (p_value=0.164). Besides, the area under the intensity curve were statistically analyzed in the two groups and there was no significant difference between two groups (p_value=0.116). As shown in the table 2, using the correlation between the results of numerical and analytical results at all angles, the correlation coefficient is greater than 0.9.

Table 3. The results of the comparison between experimental and theoretical data in all angles.

Degree	Correlation Experimental data with analytical method	P-valuefor intensity
0	0.90	0.15
30	0.90	0.12
60	0.90	0.42
90	0.91	0.37
120	0.91	0.74
150	0.92	0.74
180	0.92	0.53
210	0.91	0.10
240	0.91	0.83
270	0.91	0.17
300	0.91	0.17
330	0.90	0.38

Moreover, the forward algorithm with experimental data was evaluated and the results of this assessment can be seen in table 3.

The experimental data were compared with the theoretical values in all angles. In general, no significant difference was found between experimental and theoretical values ($p<0.01$).

4. Discussion and Conclusions

Fluorescence molecular imaging represents an extremely important advancement in non-invasive investigation of biomedical systems at the molecular level. In particular, FMT enables to derive quantitative information form three-dimensional on molecular processes in sample of interest for different biomedical research areas including pharmaceutical research. The advantage of FMT is whole body animal scanning which allows selecting one or several regions of interest without moving the animal.

FMT, which is based on appropriate forward models, predicts the propagation of photons in diffuse media like tissues. The need for a fast forward algorithm based on an analytical approach becomes ever more important for the reconstruction data to derive the concentration of fluorescent in tissues.

We have derived and validated experimentally and numerically our analytical algorithm, so PSNR, ME, and the normalized average intensity were calculated for every 30 degrees. Since the fluorescent cylinder

is 0.5 cm from the axis of the cylindrical phantom, at 180 degree, fluorescent locations were the nearest to the laser source and the highest signal was received. Then, from 0 to 180 degrees PSNR was increased. Besides, as shown in table 3, the normalized average intensity increased from 0 to 180 and this was observed in a study conducted by increasing the distance between the source and [26].Compared with numerical methods, in PSNR of the surface intensity and the area under the curve, no difference was observed between bothgroups (p_value=0.164, p_value=0.116 respectively) and the average 0.92 correlation coefficient between the two groups was confirmed by Dutta results [27] in solving the forward problem with 0.92. Average ME values which were obtained in this study were 11% in modeling of two lasers and fluorescence light. This error value is comparable with the result of a study by Ripoll [14] in modeling the laser beam with the average ME of 5%.

Since in this study the diffusion equation was used for modeling light transport in tissue, diffusion equation was evaluated again with evaluating the algorithm with experimental results. Compared with experimental results, PSNR values of these two groups were evaluated in every 30 degrees and there was no significant difference (p_value> 0.11). PSNR is one of the important parameters for an accurate modeling of the spatial distribution of fluorescence within the tissue and the results obtained demonstrate the capability of using a written algorithm in inverse problems. Besides, there was no significant difference in the area under the surface intensity curve of the sample between any of the angles (p_value>0.17). Average ME values obtained in this study were 10%. The amount of error is compared by Ripoll 3% error [25] in their modeling. By considering the error in fluorescence excitation, our modeling provides better results than Ripoll et al. which can be due to considering the exact diffusion coefficient and second order reflection from the surface.

These results show an accuracy performance of a written algorithm and its ability to propagation of light through diffuse media and further in free space in the new FMT system. There are many potential consequences to this algorithm. The most obvious consequence is the reconstruction of noncontact optical tomography images. We propose that this algorithm is extended to non-homogeneous materials and more complex geometry as well as on the animals.

Reference

[1] F. Stuker, C. Baltes, K. Dikaiou, D. Vats, L. Carrara, E. Charbon, et al., "Hybrid small animal imaging system combining magnetic resonance imaging with fluorescence tomography using single photon avalanche diode detectors," Medical Imaging, IEEE Transactions on, pp. 1-1, 2011.

[2] N. Ren, J. Liang, X. Qu, J. Li, B. Lu, and J. Tian, "GPU-based Monte Carlo simulation for light propagation in complex heterogeneous tissues," Optics express, vol. 18, pp. 6811-6823, 2010.

[3] J. Sikora, A. Zacharopoulos, A. Douiri, M. Schweiger, L. Horesh, S. R. Arridge, et al., "Diffuse photon propagation in multilayered geometries," Physics in medicine and biology, vol. 51, p. 497, 2006.

[4] S. R. Arridge, M. Cope, and D. Delpy, "The theoretical basis for the determination of optical pathlengths in tissue: temporal and frequency analysis," Physics in medicine and biology, vol. 37, p. 1531, 1992.

[5] M. Schweiger and S. Arridge, "The finite-element method for the propagation of light in scattering media: frequency domain case," Medical Physics, vol. 24, p. 895, 1997.

[6] A. Gibson, J. Hebden, and S. R. Arridge, "Recent advances in diffuse optical imaging," Physics in medicine and biology, vol. 50, p. R1, 2005.

[7] M. S. Patterson, B. Chance, and B. C. Wilson, "Time resolved reflectance and transmittance for the non-invasive measurement of tissue optical properties," Applied optics, vol. 28, pp. 2331-2336, 1989.

[8] T. J. Farrell, M. S. Patterson, and B. Wilson, "A diffusion theory model of spatially resolved, steady-state diffuse reflectance for the noninvasive determination of tissue optical properties in vivo," Medical Physics, vol. 19, p. 879, 1992.

[9] D. Contini, F. Martelli, and G. Zaccanti, "Photon migration through a turbid slab described by a model based on diffusion approximation. I. Theory," Applied optics, vol. 36, pp. 4587-4599, 1997.

[10] B. W. Pogue and M. S. Patterson, "Frequency-domain optical absorption spectroscopy of finite tissue volumes using diffusion theory," Physics in medicine and biology, vol. 39, p. 1157, 1994.

[11] A. Sassaroli, F. Martelli, D. Imai, and Y. Yamada, "Study on the propagation of ultra-short pulse light in cylindrical optical phantoms," Physics in medicine and biology, vol. 44, p. 2747, 1999.

[12] R. Aronson, "Boundary conditions for diffusion of light," JOSA A, vol. 12, pp. 2532-2539, 1995.

[13] A. D. Kim, "Transport theory for light propagation in biological tissue," JOSA A, vol. 21, pp. 820-827, 2004.

[14] J. Ripoll, V. Ntziachristos, R. Carminati, and M. Nieto-Vesperinas, "Kirchhoff approximation for diffusive waves," Physical Review E, vol. 64, p. 051917, 2001.

[15] V. Ntziachristos and R. Weissleder, "Experimental three-dimensional fluorescence reconstruction of diffuse media by use of a normalized Born approximation," Optics letters, vol. 26, pp. 893-895, 2001.

[16] R. Cubeddu, A. Pifferi, P. Taroni, A. Torricelli, and G. Valentini, "A solid tissue phantom for photon migration studies," Physics in medicine and biology, vol. 42, p. 1971, 1997.

[17] H. Marjaneh, S. Florian, V. Divya, and R. Markus, "Improving the accuracy of a solid spherical source radius and depth estimation using the diffusion equation in fluorescence reflectance mode," BioMedical Engineering OnLine, vol. 9.

[18] F. Martelli, S. D. Bianco, and P. Di Ninni, "Perturbative forward solver software for small localized fluorophores in tissue," Biomedical Optics Express, vol. 3, pp. 26-36, 2012.

[19] A. Liemert and A. Kienle, "Light transport in three-dimensional semi-infinite scattering media," JOSA A, vol. 29, pp. 1475-1481, 2012.

[20] V. Ntziachristos, "Fluorescence molecular imaging," Annu. Rev. Biomed. Eng., vol. 8, pp. 1-33, 2006.

[21] G. Popescu, C. Mujat, and A. Dogariu, "Evidence of scattering anisotropy effects on boundary conditions of the diffusion equation," Physical Review E, vol. 61, p. 4523, 2000.

[22] M. Nieto-Vesperinas, Scattering and diffraction in physical optics: New York, 1991.

[23] J. Ripoll and V. Ntziachristos, "Iterative boundary method for diffuse optical tomography," JOSA A, vol. 20, pp. 1103-1110, 2003.

[24] A. Lagendijk, R. Vreeker, and P. De Vries, "Influence of internal reflection on diffusive transport in strongly scattering media," Physics Letters A, vol. 136, pp. 81-88, 1989.

[25] J. Ripoll, R. B. Schulz, and V. Ntziachristos, "Free-space propagation of diffuse light: theory and experiments," Physical review letters, vol. 91, pp. 103901-103901, 2003.

[26] A. Soubret and V. Ntziachristos, "Fluorescence molecular tomography in the presence of background fluorescence," Physics in medicine and biology, vol. 51, p. 3983, 2006.

[27] J. Dutta, S. Ahn, C. Li, A. J. Chaudhari, S. R. Cherry, and R. M. Leahy, "Computationally efficient perturbative forward modeling for 3D multispectral bioluminescence and fluorescence tomography," 2008, p. 69130.